



12 July 1996

**CHEMICAL
PHYSICS
LETTERS**

Chemical Physics Letters 256 (1996) 653–656

Near node photoelectron holography

T. Greber, J. Osterwalder

Physik Institut der Universität Zürich, Winterthurerstrasse 190, CH-8057 Zürich, Switzerland

Received 22 February 1996; revised 29 April 1996

Abstract

A new experimental geometry for photoelectron holography is proposed. It exploits the anisotropic nature of photoelectron waves. Forward scattering is suppressed in a geometry where the scattered electrons are measured close to a node of the electron source wave. As a consequence the quality of holographic reconstructions improves considerably. The fairly complex structure of the Cs-ICO-Ru(0001)-(2 × 2) phase is treated as a model case.

Holography records and reconstructs the complete geometric information of three-dimensional objects. It is a solution of the phase problem in diffraction theories, i.e. it reassembles the phase information from a measured wave field. The phase and amplitude of a scattered wave is reconstructed from the measured intensity of the object wave that interfered in the detector with a known reference wave. While holography is widely applied in optics it became a goal for electron diffraction where a short electron wavelength could provide a direct three-dimensional image of atomic structures [1].

Photoelectron diffraction (PD) and Auger electron diffraction (AED) have all prerequisites of a holographic experiment [2,3]. The electron emission process provides a coherent reference wave that interferes with the scattered object wave in the detector (see Fig. 1). Unlike in optical holography there is a handicap of strong and anisotropic scattering to overcome in electron holography.

The electron–atom interaction in the kinetic energy range of relevance ($200 < E_{\text{kin}} < 2000$ eV or $7 < k < 23 \text{ \AA}^{-1}$) is strong. For example the elastic

scattering path length of 1000 eV electrons in Cs amounts to 28 \AA . This elastic scattering path length is of the same order as the inelastic scattering path length ($\sim 10 \text{ \AA}$). Therefore multiple scattering affects electron diffraction and thus the reconstructed images [4]. More importantly the Coulomb interaction also causes the forward focusing effect where the attractive ion core predominantly scatters the electrons along the k vector of the incoming electrons. Forward focusing dominates the diffraction pattern above 500 eV kinetic energy. Since it is a zero order diffraction effect it bears no holographic information and makes holographic reconstruction difficult. The strongly anisotropic scattering cross section also causes multiple scattering to be most prominent along forward scattering directions. Thus without forward focusing the scattering would become more isotropic, the elastic scattering path length would increase and electron holography should become possible.

In order to remove the effects of forward scattering the SWIFT (scattered-wave-included Fourier transform) algorithm was developed [5]. Essentially

it corrects for the anisotropic scattering amplitude and phase shift. Like other data filtering techniques it is an a posteriori input of information and causes artifacts in the reconstructed images [6,7]. Another way of avoiding the strong scattering was proposed with an experiment using positrons since positive particles are less strongly forward scattered in matter [8].

Here we outline an experiment that fades out forward focusing. This a priori suppression of forward (and multiple) scattering is realized by a reduction of the relative weight of direct electron emission towards the detector. As a result unambiguous reconstructions of atomic structures from single scattering calculations are found by Fourier transform.

The relative weight of forward focusing is controlled by the source wave of the emitted electron which is associated with the initial state angular momentum and the photon polarization. An anisotropic source wave causes an anisotropic illumination of the crystal and suppresses forward scattering if the illumination is weak along the forward scattering i.e. detection direction. In an experiment where the angle between the detector and the incoming X-rays is kept constant [9] this condition may be maintained in the whole diffractogram.

For the case of photoemission from an atomic s level selection rules are most simple and dictate the emitted photoelectrons to describe a p-wave. For

linearly polarized light this means that no electrons are emitted along the direction of the incoming light and therefore no forward scattering (nor backscattering) will be observed here. If the detector is placed in this direction the reference wave for the recording of a hologram is missing and correspondingly no three dimensional images can be reconstructed from such data. In moving the detector away from the node of the p-wave, the weight of the reference wave can be increased up to a level where forward scattering does not dominate the diffraction process. For the case of a CO molecule the angle α of 11° between X-rays and detector was found to be best for the holographic reconstruction from C 1s ($E_{\text{kin}} = 956 \text{ eV}$) photoelectron intensities.

In Fig. 1 the intensities for a single scattering object that is illuminated by a p-wave is sketched. In order to measure the intensity in all directions above the surface either the sample or the detector and the X-ray source must be scanned. It shows (a) the standard geometry in today's photoelectron spectrometers where α lies close to the magic angle of 54° for core level photoemission spectroscopy and (b) the experimental apparatus that is proposed for suppressing forward scattering. The experiment is described as the measurement of $|\Psi_r + \Psi_o|^2$ i.e. the superposition of a reference wave Ψ_r with an object wave Ψ_o far away from the emitter. While for $\alpha = 10^\circ$ forward focusing is absent, for $\alpha = 55^\circ$ the

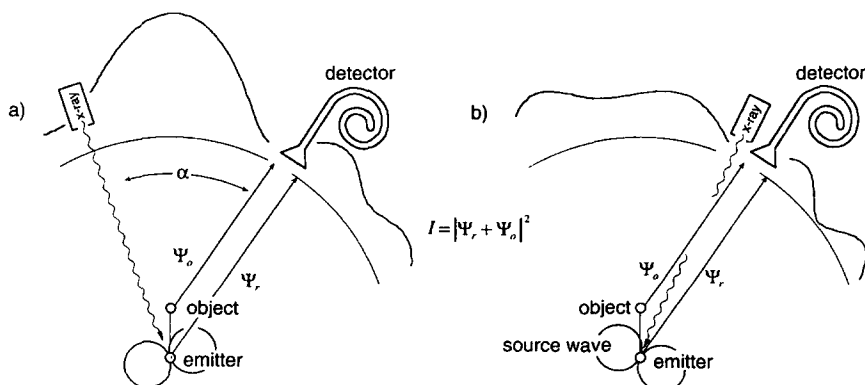


Fig. 1. Experimental apparatus for the recording of a photoelectron diffractogram. The photoemission source wave illuminates the object. The intensity $|\Psi_r + \Psi_o|^2$ of the unscattered reference wave Ψ_r and the scattered object wave Ψ_o is measured in the detector. (a) Standard geometry with an angle α between the incoming X-rays and the detector of 55° . (b) Geometry with $\alpha = 10^\circ$ where forward scattering is strongly suppressed if s-levels are excited. In order to measure the intensity over the whole surface the sample or the detector must be scanned, where it is crucial that the angle between detector and X-ray source is kept constant.

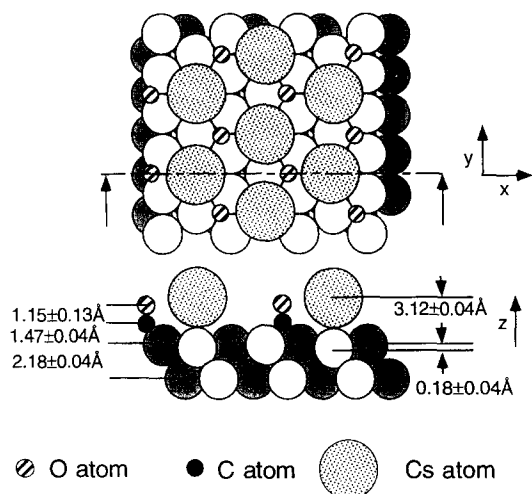


Fig. 2. Structural model and parameters for the Cs-1CO-Ru(0001)-(2 \times 2) phase as determined by LEED (cf. Ref. [10]).

intensity peaks along the axis between the emitter and the scatterer. Correspondingly higher order diffraction fringes are suppressed in the latter geometry.

In order to test the idea of near node photoelectron holography a fairly complex system, namely CO adsorbed on a monolayer of Cs on Ru(0001) was chosen. In Fig. 2 the structural parameters as found from a fully dynamical LEED analysis are displayed [10].

Diffraction patterns are calculated by means of a standard single scattering cluster (SSC) formalism [11]. This code takes the symmetry of the emitted photoelectron wave correctly into account [12]. C 1s ($E_{\text{kin}} = 956$ eV) diffraction patterns of the structure in Fig. 2 are simulated for two angles α between the incoming X-rays and the detector. Since the carbon emitters lie in the second layer single scattering is a sufficiently good description for the diffractograms. In Fig. 3a the diffractogram for $\alpha = 55^\circ$ clearly shows the forward scattering peaks along the C–Cs directions. These maxima are suppressed in Fig. 3b where the case for $\alpha = 10^\circ$ is displayed. This picture shows more interference fringes that cover the whole dynamic range though the overall intensity is about one order of magnitude weaker than in the $\alpha = 55^\circ$ case. The integrated contribution of the reference wave decreases from 98% to 53% in going from 55° to 10° . This indicates that the average interference between the reference wave and the object wave $\overline{\Psi_o \Psi_r^*}$ increases although forward scattering is suppressed. It must be noted that this argument implies as well that the $\alpha = 10^\circ$ geometry is more sensitive to structure determinations with conventional trial and error methods.

In Fig. 4 cuts in the x – z plane of Fig. 2 obtained from the holographic reconstruction of the diffractograms of Fig. 3 are shown. The reconstructions are performed by means of an algorithm that starts from

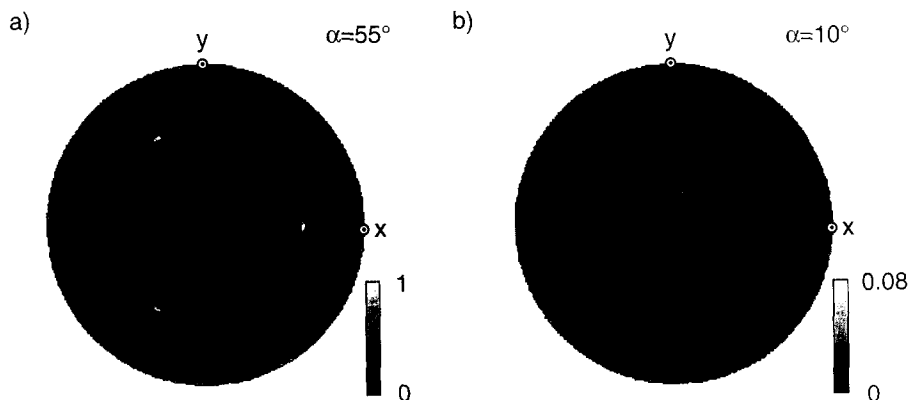


Fig. 3. Stereographically projected diffractograms representing intensities measured on the hemisphere above the sample in a linear grey scale. C 1s ($E_{\text{kin}} = 956$ eV) emission patterns were simulated by means of single scattering cluster calculations from the structure in Fig. 2. The p-polarized X-rays and the detected electrons lie in a plane normal to the polar rotation axis of the sample. (a) Standard geometry with an angle α between the incoming X-rays and the detector of 55° . (b) Geometry with $\alpha = 10^\circ$ where forward scattering is suppressed and more interference fringes can be seen.

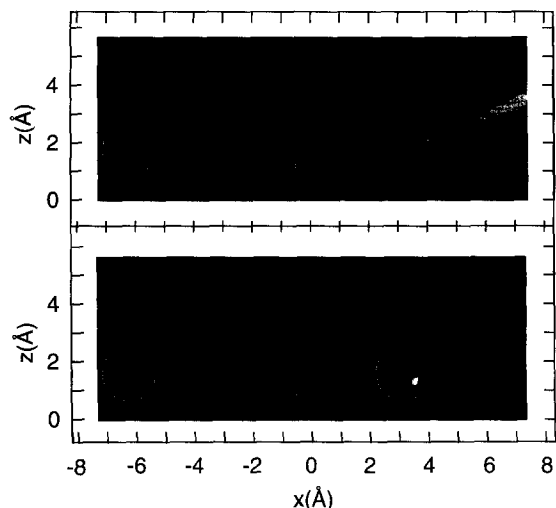


Fig. 4. Holographic reconstructions of the diffraction patterns of Fig. 3. Cuts along the $x-z$ plane containing the emitter at $(x, z) = (0, 0)$ are shown. The atomic positions from the structure in Fig. 2 correspond to the superimposed circles on the pictures. (a) With the standard geometry $\alpha = 55^\circ$ the reconstruction is dominated by the forward scattering cone originating close to the Cs atom position. (b) With $\alpha = 10^\circ$ the reconstruction clearly improves and shows peaks near the oxygen and the cesium position.

the representation of the diffractogram in spherical harmonics from where it is straightforward to do the Fourier transform that calculates the near field of the photoelectron around the emitter in real space [13].

For the case of $\alpha = 55^\circ$ forward scattering also dominates the near field and no atomic images can be reconstructed as was shown for existing experimental data sets [6,7]. This is not the case for $\alpha = 10^\circ$ where peaks near the atomic positions show up in the reconstruction. There is even an indication of the second nearest Cs atom at a distance of 6.5 \AA from the emitter. It furthermore becomes evident that the artifacts of the forward scattering cones are suppressed. Simulations without the Ru substrate indicate that the remaining artifacts in Fig. 4b) cannot be attributed to twin images of the substrate. As was done for Auger emission [14] it will be important to take the anisotropic source wave character into account in order to obtain better reconstructions.

The proposed near node photoelectron holography experiment with a constant and small emission angle relative to the node of the emitted electron wave should improve the reconstruction from diffractograms recorded at multiple energies [15,16] as well, since the forward scattering problem is also present in this kind of approach.

In conclusion, an experimental geometry that exploits the photoemission selection rules for the suppression of forward scattering is proposed. It provides single energy diffractograms that can be considered as electron holograms.

We gratefully acknowledge fruitful discussions with E. Stoll and A. Stuck.

References

- [1] D. Gabor, *Nature* 161 (1948) 777.
- [2] A. Szöke, in: *Short wavelength coherent radiation: generation and application*, eds. D.T. Attwood and J. Bocker, AIP Conf. Proc. 147 (AIP, New York, 1986).
- [3] J.J. Barton, *Phys. Rev. Letters* 61 (1988) 1356.
- [4] P. Hu and D.A. King, *Phys. Rev. B* 46 (1992) 13615.
- [5] B.P. Tonner, Z.-L. Han, G.R. Harp and D.K. Saldin, *Phys. Rev. B* 43 (1991) 14423.
- [6] A. Stuck, D. Naumovich, T. Greber, J. Osterwalder and L. Schlapbach, *Surface Sci.* 274 (1992) 441.
- [7] J. Osterwalder, R. Fasei, A. Stuck, P. Aebi and L. Schlapbach, *J. Electron Spectry. Relat. Phenom.* 68 (1994) 1.
- [8] S.Y. Tong, H. Huang and X.Q. Guo, *Phys. Rev. Letters* 69 (1992) 3654.
- [9] J. Osterwalder, T. Greber, A. Stuck and L. Schlapbach, *Phys. Rev. B* 44 (1991) 13764.
- [10] H. Over, H. Bludau, R. Kose and G. Ertl, *Phys. Rev. B* 51 (1995) 4661.
- [11] D.J. Friedman and C.S. Fadley, *J. Electron Spectry. Relat. Phenom.* 51 (1990) 689.
- [12] T. Greber, J. Osterwalder, S. Hüfner and L. Schlapbach, *Phys. Rev. B* 45 (1992) 4540.
- [13] A. Stuck, D. Naumovich, H.A. Aebischer, T. Greber and J. Osterwalder, *Surface Sci.* 264 (1992) 380.
- [14] D.K. Saldin, G.R. Harp and B.P. Tonner, *Phys. Rev. B* 45 (1992) 9629.
- [15] S.Y. Tong, H. Li and H. Huang, *Phys. Rev. Letters* 67 (1991) 3102.
- [16] J.J. Barton, *Phys. Rev. Letters* 67 (1991) 3106.